Biochemical and Biophysical Research Communications 450 (2014) 863–869

Contents lists available at ScienceDirect

Biochemical and Biophysical Research Communications

journal homepage: www.elsevier.com/locate/ybbrc

Analysis of metabolites in plasma reveals distinct metabolic features between Dahl salt-sensitive rats and consomic SS.13^{BN} rats

Le Wang [a], Entai Hou [a], Zhengjun Wang [a], Na Sun [a], Liqing He [a], Lan Chen [a], Mingyu Liang [b], Zhongmin Tian [a,*]

[a] The Key Laboratory of Biomedical Information Engineering of Ministry of Education, School of Life Science and Technology, Xi'an Jiaotong University, Xi'an 710049, China
[b] Department of Physiology, Medical College of Wisconsin, Milwaukee, WI 53226, United States

ARTICLE INFO

Article history:
Received 15 June 2014
Available online 24 June 2014

Keywords:
Hypertension
Metabolomics
Mass spectrometry
TCA cycle
Dahl salt-sensitive rats

ABSTRACT

Salt-sensitive hypertension is a major risk factor for cardiovascular disorders. Our previous proteomic study revealed substantial differences in several proteins between Dahl salt-sensitive (SS) rats and salt-insensitive consomic SS.13^{BN} rats. Subsequent experiments indicated a role of fumarase insufficiency in the development of hypertension in SS rats. In the present study, a global metabolic profiling study was performed using gas chromatography/mass spectrometry (GC/MS) in plasma of SS rats (n = 9) and SS.13^{BN} rats (n = 8) on 0.4% NaCl diet, designed to gain further insights into the relationship between alterations in cellular intermediary metabolism and predisposition to hypertension. Principal component analysis of the data sets revealed a clear clustering and separation of metabolic profiles between SS rats and SS.13^{BN} rats. 23 differential metabolites were identified ($P < 0.05$). Higher levels of five TCA cycle metabolites, fumarate, *cis*-aconitate, isocitrate, citrate and succinate, were observed in SS rats. Pyruvate, which connects TCA cycle and glycolysis, was also increased in SS rats. Moreover, lower activity levels of fumarase, aconitase, α-ketoglutarate dehydrogenase and succinyl-CoA synthetase were detected in the heart, liver or skeletal muscles of SS rats. The distinct metabolic features in SS and SS.13^{BN} rats indicate abnormalities of TCA cycle in SS rats, which may play a role in predisposing SS rats to developing salt-sensitive hypertension.

1. Introduction

Salt-sensitive hypertension plays a significant role as a factor contributing to the progression of cardiovascular diseases and affects 51% of patients with hypertension [1–3]. The mechanism underlying the development of salt-sensitive hypertension is not fully understood [4,5].

The Dahl salt-sensitive (SS) rat, a widely used model of human salt-sensitive form of hypertension, develops hypertension and renal injury upon exposure to a high-salt intake [4,6,7]. Several consomic rats have been generated by substituting a single chromosome from a normotensive Brown Norway (BN) rat for the corresponding chromosome of SS rat [8]. One of these consomic strains, the SS.13^{BN} rat, has been a valuable control strain for the study of the SS model [9,10]. Chromosome 13 of SS.13^{BN} rat is the only chromosome derived from the BN rat, which makes the SS.13^{BN} rat genetically 98% identical to the SS rat, yet exhibiting reduced blood pressure salt-sensitivity, ameliorated urinary albumin excretion and renal injury [8,11,12].

Recent studies have revealed interesting differences related to cellular metabolism between the two rat strains. Zheleznova et al. found several differentially expressed proteins in the mitochondria isolated from medullary thick ascending limb (mTAL) of kidneys in SS rats compared to SS.13^{BN} rats, including medium-chain specific acyl-CoA dehydrogenase, ATP synthase subunit alpha, acetoacetate succinyl-CoA transferase and isocitrate dehydrogenase, which indicated deficiencies in oxygen utilization in mTAL of SS rats [13].

In previous proteomic studies of SS and SS.13^{BN} rats [12], we found several dozen differentially expressed proteins, including fructose-1, insulin-like peptide 6, 6-bisphosphatase, citrate synthase, propionyl-CoA carboxylase and glutathione peroxidase. Fumarase, a key enzyme in the TCA cycle, exhibited increased abundance and lower total activity in SS rats. Subsequent sequencing, biochemical, and physiological analyses indicated a sequence variant in the fumarase gene located on chromosome 13 [14]. Furthermore, intravenous infusion of diethyl-fumarate, a fumarate precursor, could significantly exacerbated salt-induced hypertension in SS.13^{BN} rats [14]. These findings provided strong support for the association between abnormal intermediary metabolism and salt-sensitive hypertension.

* Corresponding author. Fax: +86 29 82668668.
E-mail address: zmtian@mail.xjtu.edu.cn (Z. Tian).

http://dx.doi.org/10.1016/j.bbrc.2014.06.089
0006-291X/

In the present study, plasma of SS and SS.13^{BN} rats maintained on a 0.4% NaCl diet was analyzed utilizing a GC/MS platform to explore the metabolic differences due to genetic variations between the two rat strains. We identified several differential metabolites and perturbed metabolic pathways in SS rats. In addition, TCA cycle enzyme activities were measured in several organs to gain further insights into cellular metabolic abnormalities in SS rats.

2. Methods and materials

2.1. Animals and sample collection

Rats for the experiment were bred in a specific pathogen-free animal house, maintained on a purified AIN-76A rodent diet (Dyets) containing 0.4% NaCl and had free access to water. The SS group consisted of nine rats, whereas the SS.13^{BN} group consisted of eight rats. At 8 weeks of age, rats were sacrificed with intraperitoneal injection of 10% chloral hydrate (3 ml/kg). Venous blood was collected from the vena cava in a clean tube with EDTA, then immediately centrifuged at 3000*g* for 10 min. The resulting plasma was transferred into a clean tube and stored at −80 °C until use. Livers, skeletal muscles and hearts were flushed with cold normal saline and then kept frozen at −80 °C. Animal experiments were approved by the Institutional Animal Ethics Committee of Xi'an Jiaotong University.

2.2. Measurement of blood pressure and body weight

The blood pressure of conscious rats was measured using the tail-cuff plethysmography with a computerized system (CODA-4, KENT, USA). The cuff was placed around the tail of rats and inflated to 240 mm Hg. Systolic pressure was recorded as the pressure at the point when the first tail pulse was detected. Systolic blood pressure was measured four times, every 3 min, and the average value was calculated. Heart rate was recorded at the same time. Body weights were measured at eight weeks of age.

2.3. Sample preparation and derivatization

The extraction of low molecular weight metabolites in plasma was performed according to the method described in a previous report [15] with minor modifications. 50 μl of plasma was vortexed after being spiked with three internal standard solutions (5 μl of L-2-chlorophenylalanine in water, 1 mmol/L; 5 μl of isopropylmalic acid in water, 1.1 mmol/L; 5 μl of heptadecanoic acid in methanol, 3.7 mmol/L). The mixed solution was extracted with 150 μl methanol/chloroform (volume:volume: 3:1), before being vortexed for 30 s. After storing for 10 min at −20 °C, the samples were centrifuged at 12,000*g* for 10 min. An aliquot of 150 μl of the supernatant was transferred to a clean tube, before being lyophilized using Alpha 1-2 LD plus Freeze dryer (Christ, Osterode am Harz, Germany). Samples were then derivatized using a two-step procedure [16]. For oximation, 80 μl of 239 mmol/L methoxyamine hydrochloride (Sigma–Aldrich) dissolved in pyridine were mixed with a lyophilized sample, and kept at 37 °C for 90 min. Then, 80 μl of N,O-bis(trimethylsilyl)-trifluoroacetamide (BSTFA) with 1% TMCS (Sigma–Aldrich) were added for derivatization, and heated to 70 °C for 60 min.

2.4. GC/MS analysis

A 1.0 μl of the derivatized extract was injected in splitless mode into a 7890A GC/5975C Inert MSD (Agilent Technologies, Wilmington, DE), coupled with a DB-5 column (30 m∗0.25 mm i.d.; film thickness: 0.5 μm; Agilent J&W Scientific, USA). The GC temperature programming was set to 2 min isothermal heating at 80 °C, followed by 10 °C/min oven temperature ramps to 120 °C, 4 °C/min to 260 °C, and then increased at a rate of 10 °C/min to 300 °C, where it was held for 3 min. The inlet temperature was kept at 260 °C and ion source temperature was 200 °C. Helium was used as carrier gas at a constant flow rate of 1 ml/min. Electron impact ionization (70 eV) at full scan mode (m/z 30–600) was used.

2.5. Data analysis and compound identification

The chromatogram acquisition, detection of mass spectral peaks, and their wave form processing were performed using the MSD Chemstation software E.02.02 (Agilent Technologies, Santa Clara, USA). The mass fragmentation patterns were compared with the NIST/EPA/NIH Mass Spectral Library 2011 (NIST11, Gaithersburg, MD, USA). A series of 32 reference substances were analyzed to confirm the results. Retention indexes were calculated relative to n-alkane standards under the same chromatographic conditions. The results were analyzed using MPP Version 2.1.5 (Agilent.Co) for data pretreatment procedures. The dataset for the multiple multivariate data analysis was mean centered by square root of the standard deviation of the original variables. Internal standards were used for data quality control (reproducibility). Then, the internal standards and any other known artificial peaks, such as peaks caused by noise, column bleed and BSTFA derivatization procedure, were removed from the data set. The data set was normalized using the sum intensity of the features appeared in all samples. Principal component analysis (PCA) and partial least squares discriminant analysis (PLS-DA) were used to give an overview on the separation between the different groups. Differential metabolites between the two strains of rat were identified by the non parametric Mann–Whitney-Wilcoxon test. Benjamini & Hochberg procedure was executed for controlling the false discovery rate (FDR) of a family of hypothesis tests [17]. A probability (*P*) value of less than 0.05 was considered significant.

2.6. Targeted measurement of plasma pyruvate, citrate, and fumarate

The concentration of plasma pyruvate was measured using assay kit (Jiancheng, Nanjing, Jiangsu, China) with microplate format. To determine citrate and fumarate levels in plasma, a LC/MS analysis was performed according to the method described in a previous report [15] with minor modifications. A volume of 600 μl of methanol was added to 200 μl of plasma with 10 μl of isopropylmalate in water (1.1 mmol/L) as internal standard. After vortexing, the mixture was set aside at −20 °C for 10 min and then centrifuged at 15,000*g* for 10 min at 4 °C. A 5.0 μl of the supernatant was injected into 1200–6520 Q-TOF electrospray mass spectrometer (Agilent, Santa Clara, CA), coupled with a 2.1 × 150 mm Hypersil Gold C18 column (Thermo Electron, Waltham, MA). Mobile phase A was water with 0.1% v/v formic acid while mobile phase B was methanol modified with 0.1% v/v formic acid. Gradient elution started with 2% B for 7 min and increased to 100% B over 7–21 min, then held at 100% B for 7 min. The flow rate was 0.2 ml/min. Spectra were collected in negative ESI mode over a mass range of 50–1100 amu and capillary was 3 kV. The accurate molecular weight of citrate and fumarate was first achieved using standard substance, and then the target peak areas in samples were calculated by extract ion chromatography (EIC) and normalized by the area of isopropylmalate.

2.7. TCA cycle enzyme activities assays

TCA cycle enzyme activities were measured according to the methods described in previous reports [18–23]. Liver, skeletal muscles and heart tissue specimens were homogenized extensively in a

cold HEPES solution (20 mM, pH 7.4, volume:weight: 3:1). The homogenate was centrifuged at 4 °C, 12,000*g* for 10 min. Protein concentrations of the extracts were measured using BCA protein assay kit (Beyotime, China). 2–5 μl samples of homogenate were added to initiate the reaction. Enzyme activities were determined by triplicate assays per preparation.

3. Results

3.1. Physiological parameters of the rats

All rats were maintained on a 0.4% NaCl diet until eight weeks, and appeared healthy with normal physiological activities at the beginning of blood pressure measurement. Systolic blood pressure, heart rate and body weight did not show significant differences between SS and SS.13^{BN} groups (Table 1).

Table 1
Physiological parameters of the rats.[a]

	SBP (mm Hg)	Weight (g)	Heart rate (beats/min)
SS.13^{BN} (n = 8)	138.6 ± 4.8	345.3 ± 19.3	373.2 ± 59.8
SS (n = 9)	147.3 ± 12.6	321.8 ± 17.1	406.3 ± 65.2

[a] Values are means ± SD.

3.2. Plasma metabolic profiles between SS rats and SS.13^{BN} rats

After deconvolution and excluding internal standards, the low-molecular-weight compounds in plasma were identified (listed in Supplemental Table S1). Raw analytical data were mean centered and unit variance scaled. Since variables often have very different numerical ranges, multivariate data analysis was used for the detection of variations in the levels of low concentration metabolites. Fig. 1A showed an overview of the entire set of observations for SS and SS.13^{BN} rats by principal component analysis (PCA). The data were reduced into the low-dimensional plane to visualize variations of metabolic patterns, and a PCA 3-D scores plot using 4 components ($R^2X = 0.363$, $Q^2 = 0.288$) was constructed. Differences in the metabolite spectra were readily observed between the two rat strains. The data of experimental and control group exhibited distinct trajectory. To obtain improved model transparency and interpretability, we used PLS-DA method to maximize

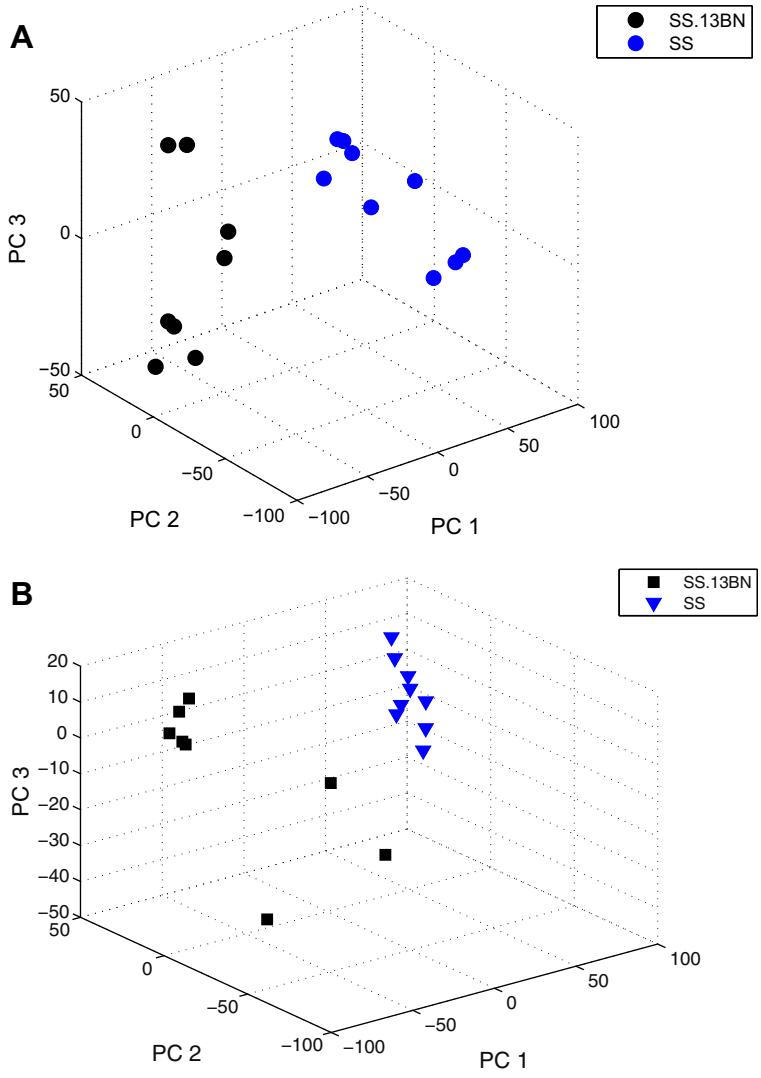

Fig. 1. SS and SS.13^{BN} rats exhibited distinct metabolic profiles. (A) PCA 3-D sores plot based on the metabolic profiling data obtained from plasma of SS rats and SS.13^{BN} rats. The black spheres indicate SS.13^{BN} rats, and blue spheres indicate SS rats. (B) PLS-DA 3-D sores plot based on the metabolic profiling data obtained from plasma of SS rats and SS.13^{BN} rats. The black squares indicate SS.13^{BN} rats, and blue triangles indicate SS rats. (For interpretation of the references to color in this figure legend, the reader is referred to the web version of this article.)

Table 2
Differential plasma metabolites between SS rats and SS.13^{BN} rats.

Compound	*P*-value [b]	Regulation	Fold change [c]	Retention index
Pyruvic acid [a]	1.68E−02	Up	1.31	1050.7
L-Lactic acid	2.44E−02	Up	1.09	1059.1
Glycolic acid	3.85E−05	Down	−3.14	1071.8
L-Valine [a]	1.29E−02	Up	1.06	1204.6
Urea	1.56E−02	Up	1.12	1239.0
L-Isoleucine [a]	1.08E−03	Up	5.62	1281.3
Glycine [a]	1.27E−02	Down	−1.41	1296.7
Succinic acid [a]	4.65E−02	Up	1.68	1304.0
Glyceric acid [a]	7.87E−03	Down	−1.16	1315.1
Fumaric acid [a]	3.89E−05	Up	1.42	1339.2
Decanoic acid	1.93E−02	Down	−5.19	1448.2
L-Methionine [a]	1.43E−03	Up	1.13	1506.8
L-Glutamic acid [a]	3.47E−03	Down	−1.43	1614.4
Pyrophosphate	7.21E−18	Down	−6.55	1645.5
L-Asparagine [a]	4.90E−02	Down	−1.77	1656.9
cis-Aconitic acid	7.71E−09	Up	5.99	1737.1
O-phosphocolamine	1.09E−02	Down	−1.07	1769.2
3-Phosphoglyceric acid	1.18E−03	Down	−2.64	1791.7
Isocitric acid [a]	6.32E−04	Up	8.00	1803.8
Citric acid [a]	4.05E−08	Up	1.52	1804.2
L-Tyrosine [a]	5.30E−03	Down	−1.07	1924.9
Hexadecanoic acid [a]	4.75E−02	Down	−1.56	2035.4
Docosanoic acid	2.44E−02	Down	−3.36	2629.3

[a] Metabolites confirmed by measuring reference substances.
[b] *P* values were calculated by the Mann–Whitney nonparametric *U* test.
[c] Fold changes were calculated as ratio of arithmetic mean values of the relative peak intensity from each group. Positive, SS/SS.13^{BN}; negative, SS.13^{BN}/SS. "Up" or "Down" means the trend of regulation for these metabolites in SS rats versus SS.13^{BN} rats, respectively.

the differences between groups. Fig. 1B depicted the 3D-scores plots for PLS-DA ($R^2X = 0.302$, $R^2Y = 0.92$, $Q^2Y = 0.807$). A better separation than those for PCA was observed, combining covariance and correlation for the variables in the two groups. The control group (SS.13^{BN} rats) presented low degree of variation, although three samples were further from the class center. The experimental group (SS rats) exhibited an overlapped clustering. This classification model further verified the robustness of the metabolomic pattern, and indicated metabolic modifications in SS rats, which might be direct or indirect effects of genetic differences on the substituted chromosome 13.

3.3. Metabolic features of SS rats

Once differences between metabolic patterns had been established, further identification of metabolites responsible for divergent metabolic profiles was performed. 23 differential metabolites were identified in the plasma (Mann–Whitney test, $P < 0.05$), including organic acids, amino acids and fatty acids. A few intermediates involved in TCA cycle were observed to show a rising tendency in plasma of SS rats, including *cis*-aconitate, isocitrate, citrate, succinate and fumarate (Table 2). Pyruvate, an important link between glycolysis and TCA cycle, was up-regulated in SS rats. An elevation of lactate suggested an association with anaerobic glycolysis. Furthermore, molecules involved in biosynthetic pathways, in which intermediates leave TCA cycle to be converted primarily to glucose, fatty acids or non-essential amino acids [24], were also different between the two groups. Valine, isoleucine and methionine showed a tendency to increase in SS rats, whereas lower levels of glutamate, asparagine, glycine and tyrosine were observed. In addition, SS rats contained higher levels of hexadecanoic acid (16:0) and docosanoic acid (22:0), which were involved in biosynthesis of unsaturated fatty acids. Several other metabolites were also detected in the SS group (Table 2), such as glyceric acid, pyrophosphate and O-phosphocolamine, respectively involved in glycerolipid metabolism, oxidative phosphorylation, phospholipid metabolism.

3.4. Verification of GC/MS results

To verify the results by GC/MS, the level of pyruvate, citrate and fumarate in plasma was measured using different methods. The plasma level of pyruvate was markedly higher in SS rats than SS.13^{BN} rats using a colorimetric method, which was in accordance with the result of GC/MS (Fig. 2A). In LC/MS analysis, m/z 191.0192 was used for extract ion of citrate and m/z 115.0104 for fumarate, coupled with correction in retention time. Consistent with the result of GC/MS, both citrate and fumarate were elevated in SS rats (Fig. 2B and C), with fold change of 1.42 and 1.70 ($n = 8–9$, $P < 0.05$) respectively. The results confirmed the accuracy of GC/MS analysis for the detection of variations in the levels of low concentration metabolites, which were difficult to detect with traditional methods, yet are often important biomarkers and indicators of metabolic defects.

3.5. Changes in activities of the TCA cycle enzyme

The observed rise of five TCA cycle intermediates (*cis*-aconitate, isocitrate, citrate, succinate and fumarate) and related metabolic differences in plasma of SS rats suggest the presence of TCA cycle abnormalities in SS rats. To obtain further insights into the TCA cycle in SS rats, we analyzed the activities of eight enzymes related to TCA cycle in heart, liver and skeletal muscles of the rats ($n = 4$), using colorimetric method. The activities of aconitase (ACON) and α-ketoglutarate dehydrogenase (KGD) were lower in the liver of SS rats compared to SS.13^{BN} rats (Fig. 3A and B). Similarly, lower levels of activities of ACON and KGD were observed in skeletal muscle and heart of SS rats, respectively. Most importantly, the activities of succinyl-CoA synthetase (SCS) and fumarase (FH) significantly decreased in all three tested organs of SS rats (Fig. 3E, F) Lactate dehydrogenase (LDH) activity was increased in the heart of SS rats

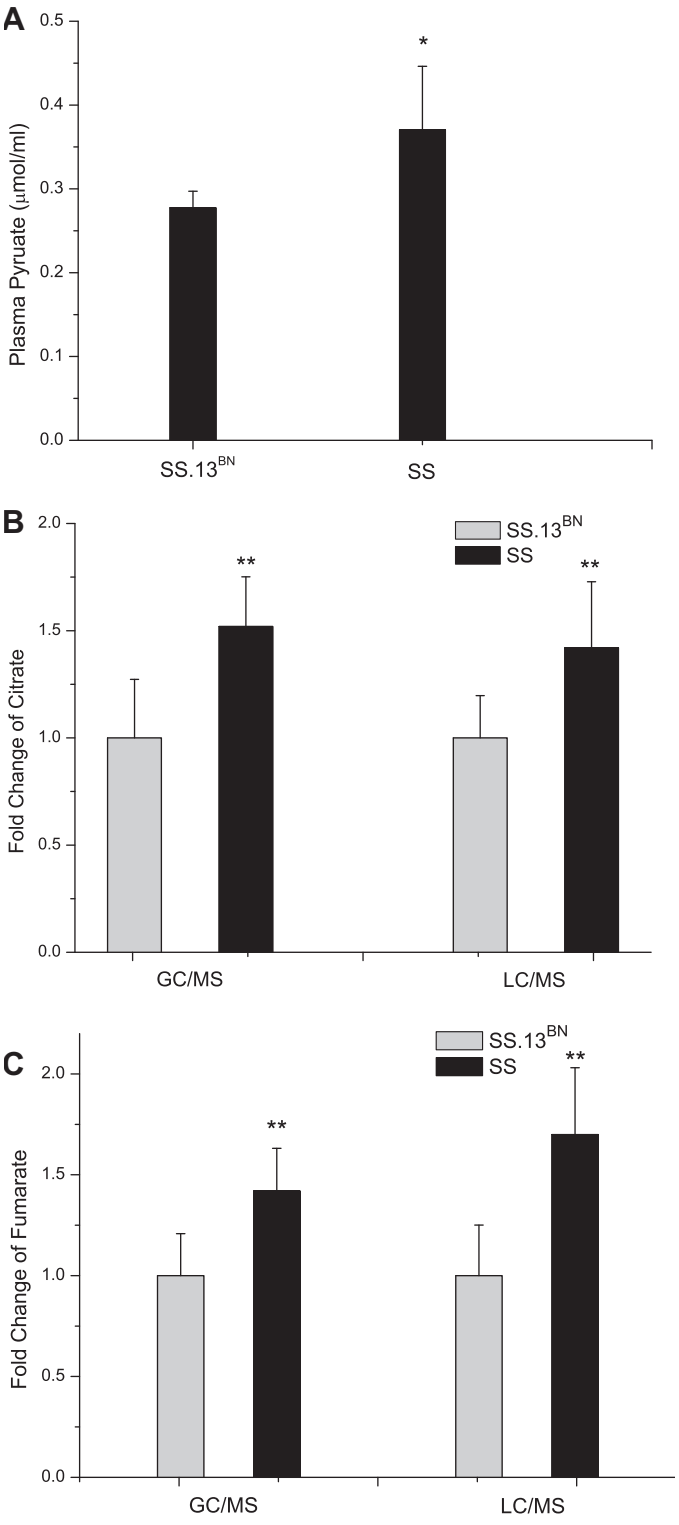

Fig. 2. Verification of GC/MS results with a second method. Plasma levels of pyruvate (A), citrate (B), and fumarate (C) were found to be higher in SS rats ($n = 9$) than in SS.13^{BN} rats ($n = 8$) using two analytical methods. $^{*}P < 0.05$, $^{**}P < 0.01$, based on two-tailed t-test; bars are means ± SD.

(Fig. 3C), whereas no difference was observed in liver and skeletal muscles. Activities of malate dehydrogenase (MDH), NAD^{+}-isocitrate dehydrogenase (NAD^{+}-ICD), NADP^{+}-isocitrate dehydrogenase (NADP^{+}-ICD) did not exhibit significant differences between the two rat strains (Fig. 3D, G, H). Fig. 4 summarized the distinct TCA cycle in SS rats compared to SS.13^{BN} rats.

4. Discussion

The present study was one of the first metabolomic studies comparing any models with different levels of blood pressure salt-sensitivity. The experimental animals were maintained on a 0.4% NaCl salt, and did not show any significant differences in heart rate, blood pressure or body weight. Thus, the differences in metabolic profiles that we detected between SS and SS.13^{BN} rats were unlikely to be secondary effects of hypertension or gross variations in overall energy intake and expenditure. Instead, the distinct metabolomic profiles between SS rats and SS.13^{BN} rats were likely direct or indirect results of genetic differences between the two rat strains, and might contribute to predisposing SS rats to developing hypertension once they are exposed to high salt diets.

Five TCA cycle-related molecules, *cis*-aconitate, isocitrate, citrate, succinate and fumarate, were significantly increased in SS rats. TCA cycle is central to the cell metabolism and the regulation of energy homeostasis [25]. In our previous studies, the kidneys of SS rats were found to exhibit insufficiencies in fumarase (FH), an important component of the TCA cycle. The resulting accumulation of its substrate, fumarate, appeared to exacerbate salt-induced hypertension based on infusion experiments performed in SS.13^{BN} rats [12,14]. The presence of an abnormal TCA cycle in SS rats was further supported by a comprehensive analysis of the activities of eight TCA cycle enzymes in heart, liver and skeletal muscles. Several of these enzymes showed lower activities in one or more organs analyzed in SS rats, consistent with our previous study of fumarase in the kidney [14]. Although it is unlikely that these changes in enzyme activities could fully account for the differentiation in plasma metabolic profiles, it confirmed general abnormalities in TCA cycle of SS rats. The abnormalities of TCA cycle might contribute to predisposing SS rats to developing tissue injury and hypertension once the rats are exposed to high salt diets, which is consistent with our previous findings [12,14,26].

Glycolysis works with the TCA cycle to fully oxidize glucose and supply energy for the body. The core part of glycolysis is the conversion of three-carbon compounds from glyceraldehyde-3-phosphate to pyruvate. 3-phosphoglyceric acid, the intermediate metabolite between glyceraldehyde-3-phosphate and pyruvate, was significantly decreased in SS rats, whereas an increased level of pyruvate with a fold change of 1.31 was observed in SS rats (Table 2 and Fig. 4). Pyruvate is an important intermediate in glucose metabolism, connecting glycolysis with the TCA cycle. A decline in 3-phosphoglyceric acid coupled with increased pyruvate raised the possibility of abnormal glycolysis in SS rats. Plasma lactate levels are the result of a finely tuned interplay of factors that affect the balance between its production and clearance. When the oxygen supply does not match its consumption, organisms were forced to produce ATP through alternative mechanisms [27]. SS rats showed higher levels of plasma lactate and higher LDH enzyme activities in the heart, which might be an attempt to compensate for insufficiencies in TCA cycle. Moreover, a higher expression of ATP synthase subunit alpha has been observed in mTAL mitochondria of SS rats [13], suggesting attempts to compensate for the TCA cycle insufficiency might occur in mitochondria as well.

It remains to be determined whether cataplerosis and anaplerosis, in which 4- and 5-carbon intermediates are extracted from TCA cycle for biosynthesis and replenished, respectively, contribute to the observed differences in TCA cycle intermediates or disease phenotypes between the two rat strains. One possibility is that asparagine was consumed to produce oxaloacetate for continuing function of TCA cycle based on low level of asparagine in plasma of SS rats compared with SS.13^{BN} rats. However, the possibility needs to be tested in future experiments.

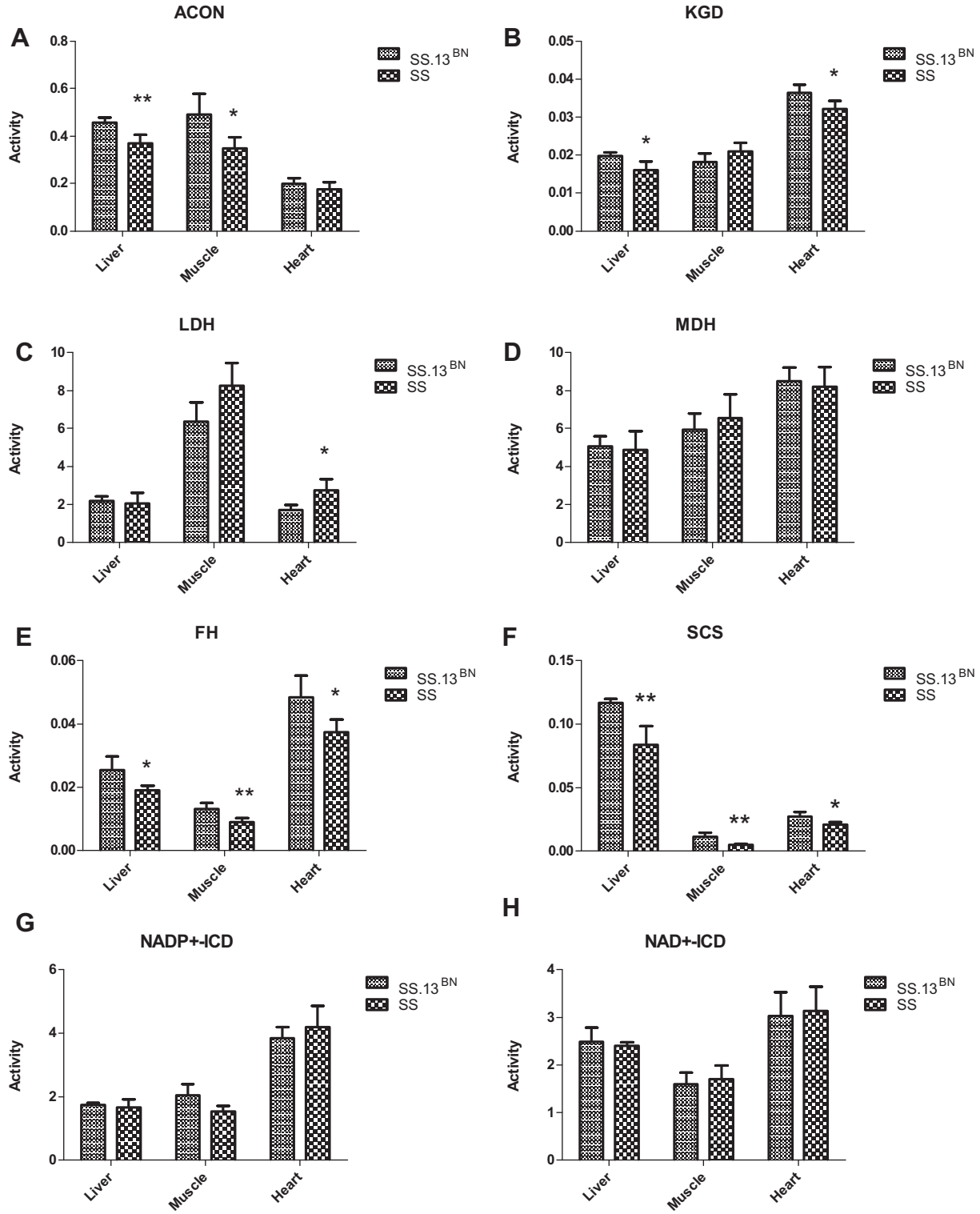

Fig. 3. TCA cycle enzyme activities in liver, skeletal muscle and heart from SS.13^{BN} rats and SS rats. A, ACON (μmol aconitate/min/mg); B, KGD (μmol NADH/min/mg); C, LDH (μmol NADH/min/mg); D, MDH (μmol NADH/min/mg); E, FH (μmol fumarate/min/mg); F, SCS (μmol succinyl-CoA/min/mg); G, NADP$^+$-ICD (μmol NADPH/min/mg); H, NAD$^+$-ICD (μmol NADH/min/mg). Enzyme activities were determined by triplicate assays per preparation ($n = 4$). Statistically significant alterations are indicated by an asterisk, $^*P < 0.05$, $^{**}P < 0.01$, based on a t-test.

It has been reported that the prevalence of salt-sensitive hypertension is significantly higher in patients with metabolic syndrome than those without metabolic syndrome [28]. SS rats have higher values for plasma triglyceride and insulin concentration, associated with a defect in insulin-stimulated glucose uptake by isolated adipocytes [29]. Accumulation of succinate in the local tissue environment appears to be an important early mechanism by which cells detect and respond to hyperglycemia [30]. The relationship between the apparently insufficient TCA cycle and lipid and other aspects of metabolism in SS rats remains to be examined.

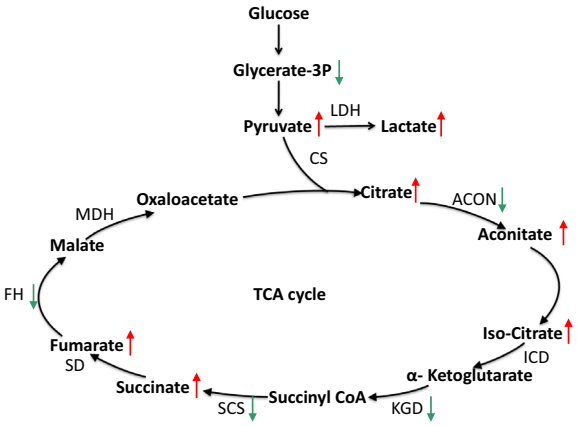

Fig. 4. Alterations related to TCA cycle in SS rats compared with SS.13^{BN} rats. Red represents up-regulated metabolites or increased enzyme activities, and green represents down-regulated metabolites or decreased enzyme activities. The levels of citrate, aconitate, isocitrate, succinate, fumarate and pyruvate, lactate were increased in plasma of SS rats, whereas glyceric acid-3P decreased. The activities of ACON, KGD, SCS and FH were significantly decreased in the heart, live, skeletal muscle, or kidneys of SS rats. (For interpretation of the references to color in this figure legend, the reader is referred to the web version of this article.)

Grants

This study was supported by the National Natural Science Foundation of China (NSFC) (Grant No. 31071029, 81270767, 81228002) and the US National Institutes of Health (Grant No. HL116264).

Disclosures

The authors declared no conflict of interest.

Acknowledgments

The authors are very grateful to Xi'an Analytical and Monitoring Centre for Agri-Food Quality Safety (Xi'an 710077, China) for the optimization of gas chromatography/mass spectrometry.

Appendix A. Supplementary data

Supplementary data associated with this article can be found, in the online version, at http://dx.doi.org/10.1016/j.bbrc.2014.06.089.

References

[1] M.H. Weinberger, J.Z. Miller, F.C. Luft, C.E. Grim, N.S. Fineberg, Definitions and characteristics of sodium sensitivity and blood pressure resistance, Hypertension 8 (1986) II127–II134.
[2] A. Morimoto, T. Uzu, T. Fujii, M. Nishimura, S. Kuroda, S. Nakamura, T. Inenaga, G. Kimura, Sodium sensitivity and cardiovascular events in patients with essential hypertension, Lancet 350 (1997) 1734–1737.
[3] A. Miyoshi, H. Suzuki, M. Fujiwara, M. Masai, T. Iwasaki, Impairment of endothelial function in salt-sensitive hypertension in humans, Am. J. Hypertens. 10 (1997) 1083–1090.
[4] B. Joe, J.I. Shapiro, Molecular mechanisms of experimental salt-sensitive hypertension, J. Am. Heart Assoc. 1 (2012).
[5] A.W. Cowley, The genetic dissection of essential hypertension, Nat. Rev. Genet. 7 (2006) 829–840.
[6] Kathleen.M. Lukaszewicz, Julian.H. Lombard, Role of the CYP4A/20-HETE pathway in vascular dysfunction of the Dahl salt-sensitive rat, Clin. Sci. 124 (2013) 695–700.
[7] J.P. Rapp, Dahl salt-susceptible and salt-resistant rats. A review, Hypertension 4 (1982) 753–763.
[8] M. Liang, N.H. Lee, H. Wang, A.S. Greene, A.E. Kwitek, M.L. Kaldunski, T.V. Luu, B.C. Frank, S. Bugenhagen, H.J. Jacob, A.W. Cowley, Molecular networks in Dahl salt-sensitive hypertension based on transcriptome analysis of a panel of consomic rats, Physiol. Genom. 34 (2008) 54–64.
[9] N. Li, L. Chen, R.W. Muh, P.-L. Li, Hyperhomocysteinemia associated with decreased renal transsulfuration activity in Dahl S rats, Hypertension 47 (2006) 1094–1100.
[10] S.A. Nonas, L.M. Vinasco, S.F. Ma, J.R. Jacobson, A.A. Desai, S.M. Dudek, C. Flores, P.M. Hassoun, L. Sam, Q.Y. Shui, Use of consomic rats for genomic insights into ventilator-associated lung injury, Am. J. Physiol. Lung Cell. Mol. Physiol. 293 (2007) L292–L302.
[11] A.W. Cowley Jr., R.J. Roman, M.L. Kaldunski, P. Dumas, J.G. Dickhout, A.S. Greene, H.J. Jacob, Brown Norway chromosome 13 confers protection from high salt to consomic Dahl S rat, Hypertension 37 (2001) 456–461.
[12] Z. Tian, A.S. Greene, K. Usa, I.R. Matus, J. Bauwens, J.L. Pietrusz, A.W. Cowley, M. Liang, Renal regional proteomes in young Dahl salt-sensitive rats, Hypertension 51 (2008) 899–904.
[13] N.N. Zheleznova, C. Yang, R.P. Ryan, B.D. Halligan, M. Liang, A.S. Greene, A.W. Cowley Jr., Mitochondrial proteomic analysis reveals deficiencies in oxygen utilization in medullary thick ascending limb of Henle in the Dahl salt-sensitive rat, Physiol. Genom. 44 (2012) 829–842.
[14] Z. Tian, Y. Liu, K. Usa, D. Mladinov, Y. Fang, X. Ding, A.S. Greene, A.W. Cowley, M. Liang, Novel role of fumarate metabolism in Dahl-salt sensitive hypertension, Hypertension 54 (2009) 255–260.
[15] W.B. Dunn, D. Broadhurst, P. Begley, E. Zelena, S. Francis-McIntyre, N. Anderson, M. Brown, J.D. Knowles, A. Halsall, J.N. Haselden, A.W. Nicholls, I.D. Wilson, D.B. Kell, R. Goodacre, Procedures for large-scale metabolic profiling of serum and plasma using gas chromatography and liquid chromatography coupled to mass spectrometry, Nat. Protocols 6 (2011) 1060–1083.
[16] J.M. Halket, Chemical derivatization and mass spectral libraries in metabolic profiling by GC/MS and LC/MS/MS, J. Exp. Bot. 56 (2004) 219–243.
[17] Y. Benjamini, Y. Hochberg, Controlling the false discovery rate: a practical and powerful approach to multiple testing, J. Royal Stat. Soc. Series B (Methodological) (1995) 289–300.
[18] C.P. Henson, W. Cleland, Purification and kinetic studies of beef liver cytoplasmic aconitase, J. Biol. Chem. 242 (1967) 3833–3838.
[19] J. Robinson, L. Brent, B. Sumegi, P. Srere, An Enzymatic Approach to the Study of the Krebs Tricarboxylic Acid Cycle, Mitochondria, A Practical Approach, IRL Press, Oxford, 1987, pp. 160–161.
[20] S. Cha, R. Parks, Succinic thiokinase I. Purification of the enzyme from pig heart, J. Biol. Chem. 239 (1964) 1961–1967.
[21] B. Ackrell, E.B. Kearney, T.P. Singer, Mammalian succinate dehydrogenase, Methods Enzymol. 53 (1978) 466.
[22] C.S. Yarian, D. Toroser, R.S. Sohal, Aconitase is the main functional target of aging in the citric acid cycle of kidney mitochondria from mice, Mech. Ageing Dev. 127 (2006) 79–84.
[23] B.t. Crabtree, E. Newsholme, The activities of phosphorylase, hexokinase, phosphofructokinase, lactate dehydrogenase and the glycerol 3-phosphate dehydrogenase in muscles from vertebrates and invertebrates, Biochem. J. 126 (1972) 49–58.
[24] O.E. Owen, The key role of anaplerosis and cataplerosis for citric acid cycle function, J. Biol. Chem. 277 (2002) 30409–30412.
[25] H. Krebs, The history of the tricarboxylic acid cycle, Perspec. Biol. Med. 14 (1970) 154.
[26] M.Y. Liang, Hypertension as a mitochondrial and metabolic disease, Kidney Int. 80 (2011) 15–16.
[27] F. Valenza, G. Aletti, T. Fossali, G. Chevallard, F. Sacconi, M. Irace, L. Gattinoni, Lactate as a marker of energy failure in critically ill patients: hypothesis, Crit. Care 9 (2005) 588.
[28] T. Fujita, Aldosterone in salt-sensitive hypertension and metabolic syndrome, J. Mol. Med. 86 (2008) 729–734.
[29] G.M. Reaven, J. Twersky, H. Chang, Abnormalities of carbohydrate and lipid metabolism in Dahl rats, Hypertension 18 (1991) 630–635.
[30] J. Peti-Peterdi, High glucose and renin release: the role of succinate and GPR91, Kidney Int. 78 (2010) 1214–1217.